ASA TECHNICAL NOTE

NASA TN D-7409

TERATIVE METHODS FOR LASMA-SHEATH CALCULATIONS - PPLICATION TO SPHERICAL PROBE

y L. W. Parker and E. C. Sullivan

Goddard Space Flight Center
Greenbelt, Md. 20771

TIONAL AERONAUTICS AND SPACE ADMINISTRATION • WASHINGTON, D. C. • MARCH 1974

1. Report No.	2. Government Accession No.	3. Recipient's Catalog No.
D- 7409		

4. Title and Subtitle	5. Report Date
Iterative Methods for Plasma-Sheath Calculations - Application to Spherical Probe	MARCH - 1974
	6. Performing Organization Code 641
7. Author(s) L. W. Parker and E. C. Sullivan	8. Performing Organization Report No. G-7337
9. Performing Organization Name and Address Goddard Space Flight Center Greenbelt, Maryland 20771	10. Work Unit No. 188-48-52-05
	11. Contract or Grant No.
	13. Type of Report and Period Covered Technical Note
12. Sponsoring Agency Name and Address National Aeronautics and Space Administration Washington, D. C. 20546	14. Sponsoring Agency Code

15. Supplementary Notes

16. Abstract

The computer cost of a Poisson-Vlasov iteration procedure for the numerical solution of a steady-state collisionless plasma-sheath problem depends on (a) the nature of the chosen iterative algorithm, (b) the position of the outer boundary of the grid, and (c) the nature of the boundary condition applied to simulate a condition at infinity (as in three-dimensional probe or satellite-wake problems). Two iterative algorithms, in conjunction with three types of boundary conditions, are analyzed theoretically and applied to the computation of current-voltage characteristics of a spherical electrostatic probe. The first algorithm has been commonly used by physicists, and its computer costs depend primarily on the boundary conditions and are only slightly affected by the mesh interval. The second algorithm is not commonly used, and its costs depend primarily on the mesh interval and slightly on the boundary conditions. New current-voltage data not previously available are obtained for the spherical probe at large radius (141 Debye lengths) and large potential (100 thermal energy units), that is, large values for which computations have been considered costly.

17. Key Words (Selected by Author(s))	18. Distribution Statement
Computers, Physics, Plasma-sheath problem, Boundary-value problems	Unclassified–Unlimited
	Cat. 25

19. Security Classif. (of this report)	20. Security Classif. (of this page)	21. No. of Pages	22. Price
Unclassified	Unclassified	18	$3.00

* For sale by the National Technical Information Service, Springfield, Virginia 22151.

CONTENTS

ITERATIVE METHODS FOR PLASMA-SHEATH CALCULATIONS-APPLICATION TO SPHERICAL PROBE

L. W. Parker
Mt. Auburn Research Associates, Inc.
and
E. C. Sullivan
Goddard Space Flight Center

INTRODUCTION

The term *plasma-sheath problem* denotes any boundary-value problem described by the Poisson and steady-state Boltzmann equations. The charge density is obtained through solutions of the Boltzmann equation, assuming a fixed electrostatic potential distribution: the potential in turn is obtained by a solution of the Poisson equation assuming a fixed charge density distribution. Hence, the solutions of the two equations must be self consistent. The solutions of the Boltzmann equation are the phase-space densities of ions and electrons, which in turn lead to the respective particle densities through moment integrals. When the mean free path is finite, the phase-space density varies along the particle trajectories. When the mean free path is infinite, the Boltzmann equation becomes the Vlasov equation, where the phase-space density does not vary along a trajectory. Even in this case one must still trace the complete trajectory in order to evaluate the phase-space density. Hence, the charge density is a complicated functional of the potential distribution; that is, it depends on the potential distribution elsewhere in space, and the Poisson-Boltzmann (or Poisson-Vlasov) problem may be said to be nonlocal.

We are concerned in the present work with the solution of plasma-sheath Poisson-Vlasov systems. In general, one must formulate the problem on a grid and use iterative numerical techniques (Poisson-Vlasov iteration) to obtain self-consistent solutions.* Physicists have devised iterative methods for the numerical solution of particular plasma-sheath problems, such as those of probes (References 1 to 7), high-velocity satellite wakes (References 8 to 11), ion engines (Reference 12), and plasma diodes (References 13, 14). Among the papers cited, References 5 to 7 and 9 refer to a theoretical analysis of the iteration method; these analyses were relatively specialized to the specific problem. Although it is perhaps obvious that the various plasma-sheath problems exemplified by References 1 to 14 are related, their interrelationship and the theoretical basis of the iterative methods presented have not been studied systematically. It is felt that such a study would be valuable to workers contemplating new sheath calculations, by helping to provide a basis

*An alternate approach is that of time-sequential solution (direct computer simulation), although to date this has proved feasible only for problems with simple boundary conditions (for example, see papers by R. W. Hockney and others in *Methods in Computational Physics*, 9, B. Alder, S. Fernbach, and M. Rotenberg, eds., Academic Press, N.Y., 1970). The spherical probe problem has been approached this way by N. Albers (Stanford University SU-IPR Rpt. No. 499, December 1972)

for estimating computer costs. Preliminary results of the present investigation have been reported in Reference 15.

It should be noted that mathematicians have investigated the formal theory of iterative processes for general elliptic boundary-value problems (References 16 to 21), but have not considered their practical applications to the class of problems associated with plasma sheaths.

A unique problem arises when one boundary surface is at infinity, such as in probes (References 1 to 7) and satellite wakes (References 8 to 11). The outer boundary condition must be simulated on the computer by a necessarily artificial finite condition (for example, an assumed linear condition on the potential and/or its gradient on the surface of a large box surrounding the region of interest). This document deals primarily with such problems. In it are investigated, both by theoretical analysis and computer experiments, two iterative algorithms with respect to stability and number of iterations required. The two algorithms are complementary in that the first one depends primarily on the outer boundary condition and only slightly on the mesh interval, whereas the second one is only slightly affected by the outer boundary condition and depends primarily on the mesh interval. The first algorithm (Equation (2)) is the prototype of that which has been used apparently by most physicists (References 1, 3, 4, 6, 7, 9), but which has only recently begun to interest mathematicians (Reference 16). The second algorithm (Equation (7)) has received little practical but much mathematical attention (References 18, 19, 22, 23).

To obtain an adequate quantity of empirical numerical data with a relatively small computer expenditure, a one-space-dimensional model problem has been chosen: a spherical probe in a collisionless monoenergetic plasma (References 1, 2, 5, 7, 24). Previously, efficient numerical methods that take maximum advantage of symmetry (References 1 and 5) have been applied to this one-dimensional problem. In this paper the solution is obtained by applying a general iterative method that is insensitive to both symmetry and the number of dimensions.

FIRST ALGORITHM

It is assumed that in an arbitrary three-dimensional problem the partial differential Poisson equation has been replaced by a discrete approximation, that is, by a set of difference equations based on a chosen grid (and including a chosen outer boundary condition). The term *solution vector* is defined as that vector whose components are the values of the potential at the grid points. This solution vector satisfies a matrix equation of the form

$$L\vec{\phi} = \vec{F}(\vec{\phi}) \tag{1}$$

where L is the discrete analog of the Laplacian operator, $\vec{\phi}$ is the solution vector (potential distribution), and $\vec{F}$ consists partly of the negative of the charge-density vector whose components are the values of the charge density at the grid points. In addition, each component of $\vec{F}$ generally depends on more than one component of $\vec{\phi}$. It is assumed that

a numerical procedure is available that is capable of computing $\vec{F}$ when $\vec{\phi}$ is given; that is, the procedure obtains solutions of the Boltzmann equation leading to the charged-particle densities and the vector $\vec{F}$. Thus, $\vec{F}$ formally can be considered as resulting from a nonlinear operation on $\vec{\phi}$.*

The first of the two iterative algorithms (Equation (2)) will be discussed in detail:

$$L\vec{\phi}_{n+1} = \alpha\vec{F}(\vec{\phi}_n) + (1-\alpha)\, L\vec{\phi}_n \tag{2}$$

In this algorithm, $\vec{\phi}_n$ represents the n-th iterate for the vector $\vec{\phi}$, n denotes the iteration index, and α is a positive scalar relaxation parameter between zero and unity that couples (or mixes) successive iterates. (More generally, α can be nonstationary (dependent on n), or a diagonal matrix (dependent on position) (Reference 1).) When α is 1, there is direct iteration, which is the discrete analog of the well known Picard method of successive approximations for nonlinear two-point boundary-value problems (References 17, 18, 20, 21). When α is small, previous iterates are weighted heavily on the right-hand side of (2). It will be shown that the iteration properties of (2) depend strongly on the boundary condition. To study the growth of errors, $\vec{\epsilon}_n$ will denote an error vector (defined as the difference between $\vec{\phi}_n$ and the true solution vector). Assuming that $\vec{F}$ is differentiable, first-order linearization analysis of (2) leads to a matrix relation between the n-th and (n+1)-th error vectors:

$$\vec{\epsilon}_{n+1} = M\vec{\epsilon}_n \tag{3}$$

where the error propagator matrix M is defined by

$$M = 1 - \alpha + \alpha L^{-1} J \tag{4}$$

In (4), L^{-1} is the inverse of the operator L, and J is the Jacobian matrix of partial derivatives of the components of $\vec{F}$ with respect to the components of $\vec{\phi}$. Therefore, the iteration either converges or diverges depending on whether the spectral radius of M is less than or greater than unity. Because the Jacobian matrix is difficult to represent analytically, its effects are studied in a crude manner by introducing an equivalent scalar parameter $dF/d\phi$. For the situations of interest here, where α must be small, $dF/d\phi$ plays the role of a Lipschitzian constant (Chapter 9 of Reference 21 or p. 2 of Reference 23). This is probably justified as a zero-order approximation if the range of the eigenvalues of the Jacobian matrix is small compared with the range of the eigenvalues of L^{-1}. (Some a posteriori support will be given in the section that discusses the second algorithm.)

* The example of a spherical electrostatic probe is treated in detail in the next section.

For simplicity, a three-dimensional Dirichlet boundary-value problem contained within a large cube that is divided into N mesh intervals of uniform width h along each of the three dimensions is assumed. If the simplest centered seven-point difference scheme is used for L, the eigenvalues of L are given by simple trigonometric functions (for example, by generalizing Reference 19 or p. 230 of Reference 22 to three dimensions), and the triply-indexed eigenvalues of M become (Appendix A of Reference 6):

$$\lambda_{jk\ell} = 1 - \alpha - \alpha\left(\frac{h^2}{4}\right)\left(\frac{dF}{d\phi}\right)\left[\sin^2\frac{j\pi}{2N} + \sin^2\frac{k\pi}{2N} + \sin^2\frac{\ell\pi}{2N}\right]^{-1} \qquad (5)$$

$$(j, k, \ell = 1, \ldots\ldots, N\text{-}1)$$

According to (5), in the α, λ plane, all eigenvalues lie within a fan of straight lines with a common vertex $(\alpha, \lambda) = (0, 1)$. Let σ denote the spectral radius of M, that is, the largest eigenvalue magnitude. Then, as shown in Figure 1, σ is less than unity and the iteration converges for a restricted range of α between zero and a critical value α_c, which is controlled by the largest eigenvalue of L^{-1}. The factor by which the error is reduced after n iterations is of the order of σ^n, which for σ close to unity is given approximately by the expression $[1\text{-}n(1\text{-}\sigma)]$. For $\alpha > \alpha_c$, $\sigma > 1$, and the iteration theoretically diverges. The spectral radius $\sigma(\alpha)$ is minimized at the optimum value α_{opt}, which gives the maximum rate of convergence: the minimum number of iterations. In the range between zero and α_{opt}, the rate of convergence increases with increasing α. In this range, the dominant eigenvalue is given by the largest indices in (5) and is positive; hence, the iteration is monotone (that is, the error does not change sign in successive iterations). For $\alpha > \alpha_{opt}$, the dominant eigenvalue is given by the smallest indices in (5) and is negative; therefore, the iteration is oscillatory and the error changes sign in successive iterations. For $\alpha > \alpha_c$, the iteration not only diverges but diverges in an oscillatory fashion.

In problems with only one or two dimensions, the eigenvalues are given by an equation similar to (5), but which has only one or two terms in the parentheses instead of three. For $N \gg 1$, which is usually the case (Appendix A of Reference 6):

$$\alpha_c \cong 2\left[1 + CK\frac{dF}{d\phi}\frac{N^2h^2}{\pi^2}\right]^{-1} \qquad (6)$$

where C is the reciprocal of the number of dimensions, and K is unity for Dirichlet conditions. Note that α_c depends on Nh rather than on h (p. 159 of Reference 21), where Nh is a linear dimension across the grid, say in Debye lengths. Hence, if the linear dimensions of the grid are large in Debye lengths, so that Nh is large, then (6) shows that the range of α within which the iteration converges becomes small, that is, is bounded between zero and $\alpha_c \sim (Nh)^{-2}$. In fact, a qualitatively similar relation between convergence and grid dimensions has been observed by Laframboise (Reference 1), Parker (References 6 and 7), and Parker and Whipple (Reference 3) on probe problems (Reference 15), and by Call (Reference 10) and Maslennikov and Sigov (Reference 9) on the satellite wake problem.

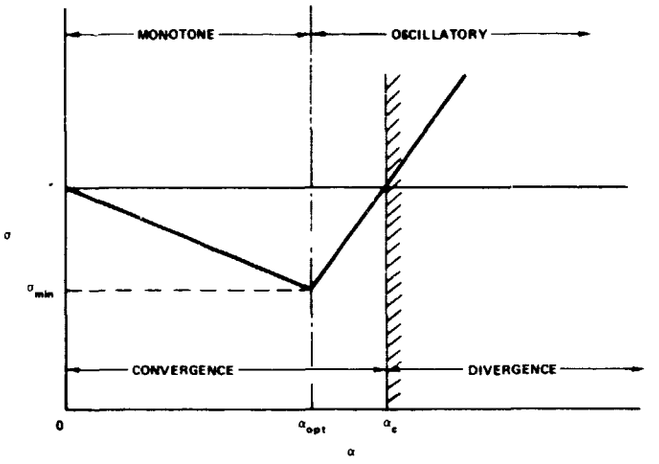

Figure 1. Spectral radius of iteration matrix for linearized problem.

Also, if the charge density has a singular character, as in the spherical probe problem to be discussed later, $dF/d\phi$ can become large, thus forcing the reduction of α still further. Finally, it is observed that as $(dF/d\phi)(Nh)^2$ becomes large, the following conditions prevail:

- α_{opt} tends to coincide with α_c while both become small.
- The iteration is monotone, and, for α within the convergent range, the spectral radius of M is controlled by the smallest eigenvalue of L^{-1} and is given by $1-A\alpha$ where $A = 1 + C\,(dF/d\phi)(h^2/4)$.
- Because $A\alpha << 1$, the reduction of error after n iterations is approximated by the expression $\exp(-An\alpha)$.
- For α even slightly larger than α_c, the iteration diverges rapidly.

Incidentally, Lettenmeyer's criterion (References 17, 18, and pp. 40 and 143 of Reference 21; the authors were not able to locate Lettenmeyer's original paper) for the convergence of the Picard procedure in the one-dimensional continuous Dirichlet problem follows immediately from (5) with $\alpha = 1$ and $N >> 1$. That is, the spectral radius is then given by $N^2h^2|dF/d\phi|/\pi^2$, which must be less than unity for convergence. This is the Lettenmeyer criterion, where $|dF/d\phi|$ is actually a Lipschitz constant.

To evaluate the role played by boundary conditions, a two-surface boundary-value problem with a Dirichlet condition on one boundary surface and a *floating* linear relation between the potential and its gradient on the other boundary is considered. This has been employed in probe problems to simulate the condition at infinity (References 1, 3 to 7, 15). The largest eigenvalue of the reciprocal matrix L^{-1} is increased by a factor $K > 1$ which appears in (6). It can be shown, by analyzing the roots of the appropriate determinantal equation (for example, Equation (1.34*) of Reference 25) for a one-dimensional problem with a

Dirichlet condition ($\phi = 0$) at one end and a floating condition ($\phi' = -k\phi$) at the other end, that $K = \pi^2/z^2$, where z is the root of $kNh = z\tan(z-\pi/2)$ lying in the range $\pi/2 \leqslant z \leqslant \pi$. That is, K goes from unity to 4 as k goes from infinity ($\phi = 0$) to zero ($\phi' = 0$). Thus, the use of a floating condition tends to require smaller values of α and correspondingly more iterations as opposed to the Dirichlet condition. The value of $dF/d\phi$ may change in such a direction as to cancel this effect. It has been observed in numerical experiments with the spherical probe (Table 1) that in some cases floating conditions converge more rapidly, and in other cases more slowly than fixed Dirichlet conditions. The value of $dF/d\phi$ is not usually predictable and is considered to be an empirically determined parameter. Nevertheless, it is a useful parameter because, from problem to problem, it varies more slowly than α_c (Table 2).

The following numerical experiments with the spherical probe model also should be relevant to three-dimensional problems. Preliminary results were reported in Reference 15.

SPHERICAL PROBE

The problem of the spherical electrostatic probe is used as the model for computational experiments involving tests of three types of numerical boundary conditions simulating the condition at infinity, and two types of Poisson-Vlasov iteration (the first and second algorithms). In particular, the monoenergetic version of the probe calculation is used, which assumes that all attracted particles have the same nonvanishing total energy E_0. Theoretical calculations of current-voltage characteristics for this model, with repelled particles assumed to be described by a Boltzmann factor (that is, an exponential function of local potential), have been made by Bohm et al. (Reference 24), Bernstein and Rabinowitz (Reference 2), and Laframboise (Reference 1). A similar model, but one using repelled as well as attracted monoenergetic particles, has been used by Guderley (Reference 5) (based on unpublished work by G. Medicus), and is the model discussed in this section. These monoenergetic models are physically justified on the basis that the problem can be solved numerically for arbitrary energy distributions (usually a Maxwellian) by summing over monoenergetic contributions (that is, by energy-quadratures). Such calculations have been done independently by Laframboise and Parker (unpublished work) duplicating results obtained earlier by Laframboise (Reference 1), who used a special method for Maxwellian energy distributions. Another justification is based on computed solutions that show that as the probe potential becomes large the monoenergetic attracted-particle current becomes identical to the Maxwellian current.

Figure 2 indicates the parameters of the probe problem, with ϕ denoting dimensionless potential in units of E_0/e, where E_0 is the singular energy (the same for both attracted and repelled particles, consisting of electrons and singly-charged ions with charge e). The unit of length is $(E_0/2\pi n_0 e^2)^{1/2}$, as in Reference 5, that is, larger than the usual Debye length by a factor of $\sqrt{2}$. The range of r is between r_p (dimensionless probe radius, where the potential is ϕ_p) and r_b, the dimensionless outer-boundary radius.

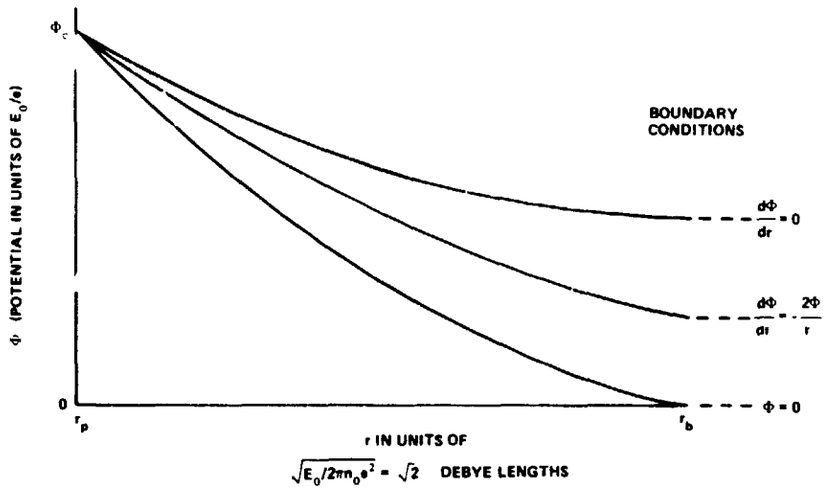

Figure 2. Spherical collisionless monoenergetic probe model: Artificial boundary conditions are established to simulate boundary condition at infinity (r_b is moved outward until current does not change).

The equations that may be used for a monoenergetic problem in which the ions and electrons both have the same energy are presented in condensed form as follows. (See References 5, 7, and 24 for derivations and more detailed discussions.)

In the Poisson equation

$$\frac{d^2\phi}{dr^2} + \frac{2}{r}\frac{d\phi}{dr} = F(\phi) = 2n(-\phi) - 2n(\phi)$$

where $n(-\phi)$ and $n(\phi)$ denote dimensionless electron and ion density, respectively. These densities are functionals of a function g(r), defined by

$$g(r) \equiv r^2(1-\phi)$$

where g(r) is proportional to the square of the largest angular momentum or impact parameter which a particle can have at point r, and is such that there is a turning-point at r (Section 4.2 of Reference 24). Minima in g, namely g_l and g_m, correspond to maxima in the effective potential and govern the density and current as seen in the following equations:

- If $g(r) > 0$ for $r_p \leq r \leq r_b$, define $g_l(r) = \underset{r' > r}{\text{Min}}\, g(r')$, $\qquad g_m = \underset{r}{\text{Min}}\, g(r) = \underset{r}{\text{Min}}\, g_l(r)$

  Then

$$n(\phi) = \frac{1}{2}\sqrt{1-\phi}\left[1 + \sqrt{1-\frac{g_m}{g}} - 2\sqrt{1-\frac{g_l}{g}}\right]$$

- If $g(r) > 0$ for $r_p < r_0 < r \leq r_b$, then

$$g_m = 0$$

$$n(\phi) = 0 \quad \text{for } r \leq r_0$$

$$n(\phi) = \sqrt{1-\phi}\left[1 - \sqrt{1 - \frac{g_1}{g}}\right] \quad \text{for } r_0 < r \leq r_b$$

- Dimensionless current density is

$$\frac{j}{j_0} = \frac{g_m}{r_p^2} \qquad (j_0 = \text{current at zero probe potential})$$

Finding the minima g_1 and g_m (where g_1 is the lowest value of g ahead of a fixed point r, and g_m is the minimum over all r) is an operation easily performed and ideal for computer calculations when the ϕ-values are defined at a set of grid points. The special radius r_0 is defined as the smallest radius such that g is positive for all $r > r_0$, and is the largest radius for which $1 - \phi$ assumes negative values. In all of the cases treated here, the g(r) for the correct solution has a single minimum at the absorption radius r_c as shown for the attracted particles in Figure 3. A typical function g(r) for the repelled particles is also shown in Figure 3 by the dashed curve, where there is a radius r_0 such that g is negative for $r < r_0$. For intermediate potential distributions occurring during iterative cycling, the function g(r) may become very complicated, but the above formulas take into account any possible variation. The formulas for monoenergetic particles are directly useful for arbitrary polyenergetic distributions by means of simple quadratures.

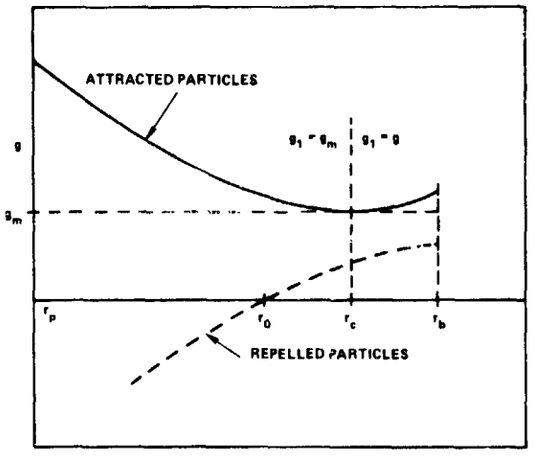

Figure 3. Special case of a nonmonotonic function g(r) with a single minimum at r_c for attracted particles. For repelled particles, g(r) may change sign (as at r_0 in dashed curve).

The quantity of interest is the current of ions or electrons collected by the probe. Since r_b cannot be infinite, the question is how large must r_b be in order to simulate sufficiently well the boundary condition at infinity where ϕ vanishes. It is found in practice that as r_b increases, the current will eventually level off and become independent of r_b. It is also found that increasing the value of r_b causes the computer cost per solution to increase, since more grid points would be required to control the truncation error, and the number of iterations would tend to increase in accord with the analysis of the preceding section.

Several different types of boundary conditions may be imposed at r_b. (Laylor (Reference 26) has studied various types of conditions with respect to how well they simulate the boundary condition at infinity; the effect of the condition on iterations was not studied.)

Three types of boundary condition studied in the present work are illustrated in Figure 2; (a) the zero-potential fixed condition, which has been used ad hoc for satellite wake calculations (References 8 to 11); (b) the inverse-square-law floating condition, which represents the proper asymptotic behavior for the probe problem, and so has been used effectively for spherical probe calculations (References 1 and 5), and (c) the zero-gradient floating condition. The zero-potential and zero-gradient conditions represent opposite-extreme conditions. General linear relations, including inverse-square and exponential laws, should give results lying between these extremes. Therefore, the three conditions studied are probably representative of the range of interest. These conditions have different properties with respect to the leveling-off value of r_b and the number of iterations required for convergence; it is of interest to determine which condition results in the smallest net computer time per solution. Therefore, the optimum values of r_b and the iteration parameters for both the first and second algorithms will be determined.

Four physical problems have been studied: probe radius r_p equal to 10 and 100 units (14.1 and 141 Debye lengths), with probe potential ϕ_p equal to 10 and 100 units for each probe radius. The extreme values of probe radius and potential were chosen because they are physically interesting and also numerically interesting, that is, likely to be costly in computer time. For each problem, all three boundary conditions were investigated to find the smallest boundary radius r_b consistent with stationary current, and the smallest number of iterations required for the first algorithm (Equation (2)). To compare numbers of iterations, the iteration was always started with the Laplace solution as a standard initial estimate. The iteration was continued until successive iterates, if they converged, differed by less than one part in 10^5 in the current density.

Results for the 12 cases are shown in Table 1. For each case, the table gives the values of four quantities: the minimum r_b for stationary current, the optimum (essentially the critical) value of α, the minimum number of iterations n_{min}, and the approximate time in seconds on an IBM 7094 computer. (Empirically, the time was about one ms/grid point/iteration.) For all but one case the mesh interval was h=1, yielding the values shown in Table 1 of dimensionless current density j/j_0, with a truncation error of the order of a few tenths of one percent, as indicated by the numbers in parentheses. For the zero-

Table i

Optimum Iterations with First Algorithm *

Conditions at r_b	r_p = 10 (14.1 Debye lengths)					r_p = 100 (141 Debye lengths)				
	Case	$r_{b\,min}$	α_{opt}	n_{min}	Time (s)	Case	$r_{b\,min}$	α_{opt}	n_{min}	Time (s)
$\phi_p = 10$	$j/j_0 = 3.44$ (–0.55%)†, $r_c = 14$					$j/j_0 = 1.90$ (–0.24%), $r_c = 108$				
$\phi = 0$	1	20	0.09	150	2	7	140	0.005	1600	65
$\phi' = -2\phi/r$	2	16	0.08	150	1	8	110	0.02	510	5
$\phi' = 0$	3	16	0 04	300	2	9	110	0.02	620	6
$\phi_p = 100$	$j/j_0 = 9.62$ (+0.14%), $r_c = 24$					$j/j_0 = 2.57$ (+[illegible]2%), $r_c = 126$				
$\phi = 0$	4	32	0.03	470	10	10	165‡	0.0003§	23 000§	590
$\phi' = -2\phi/r$	5	28	0.01	890	16	11	130	0.004	3200	95
$\phi' = 0$	6	28	0.003	2900	53	12	130	0.0025	4700	140

*Tolerance 10^{-5}; h=1 for all except Case 10.

r_b = outer boundary radius; r_p = probe radius; ϕ_p = probe potential; r_c = absorption radius.

†Truncation error.

‡Convergence could not be achieved for r_b in the range 150 to 160; hence, 165 may be somewhat high.

§This α and n for h=2.5 with error = –0.98 percent. For h=5 with error = –1.9 percent, α = 0.00045 and n = 18 000.

potential boundary condition and for $r_p = \phi_p =$ [illegible], the smallest value of h used was 2.5 because of computer-time limitations. The truncation error was estimated by running with successively smaller values of h (down to 0.1). The computer time in each case is proportional to the product of n and the number of grid points. (This is because a direct elimination method was used to solve the tridiagonal system of Poisson difference equations, so that the time per grid point is a constant for that part of the calculation.)

The boundary conditions may be assessed with respect to computer economy as follows.

- For $\phi_p = 10$ (large but not extremely large potential), the two floating conditions are comparable.
- For $\phi_p = 100$ (extremely large potential), the inverse-square floating condition is superior to the zero-gradient floating condition.
- For $r_p = 10$ (large but not extremely large radius), the fixed condition is comparable or superior to both floating conditions.
- For $r_p = 100$ (extremely large radius), the floating conditions are superior to the fixed condition.

For large probe potential or probe radius, the fixed condition has the peculiar property that, for a fixed α, as r_b increases, the number of iterations goes up and then down again. For Case 10, as noted in Table 1, convergence was essentially impossible to obtain when r_b was in a certain range of values. The floating conditions were free of such difficulties.

Table 2 presents the empirical values of $n/(Nh)^2$, $\alpha(Nh)^2$, K, and $(dF/d\phi)$ obtained from (6), where $Nh = r_b - r_p$. Throughout the table, the ratios of the largest to the smallest values of $n/(Nh)^2$, $\alpha(Nh)^2$, and $(dF/d\phi)$ are 9, 15, and 12, respectively. These factors are much smaller than the variation of α in Table 1, that is to say, by a factor of 300. For 9 out of the 12 cases, $dF/d\phi$ has values between about 1 and 3. In Cases 3, 6, and 10, $dF/d\phi$ has values of about 5, 7, and 16, respectively. The occurrence of these larger values is probably connected with the existence of a singularity in the derivative of the density as a function of potential (where a radicand vanishes).

If the error reduction by iteration is described by the expression $\exp(-Bn\alpha)$, the empirical coefficient B is found sometimes to be less than unity, in contradiction to the linearization theory. This is probably due to the closeness of the spectral radius σ to unity, so that $1-\sigma$ is sensitive to small perturbations in the theory. For example, the neglect in the spread of the eigenvalues of the Jacobian matrix J could lead to such a perturbation. This affects the number of iterations. However, the critical value of α is much less affected. Indeed, consistent with the theory, α_c is found to be a decreasing function of Nh, and is insensitive to h for a given Nh.

Aside from the properties of the iteration process, Table 1 shows that the minimum value of r_b is larger for the fixed condition than for the two floating conditions, but is independent of which floating condition is used. This is consistent with References 1 and 26. Moreover, the minimum r_b is found to be independent of h (not indicated in Table 1).

Table 2

Correlation* of n, α, $dF/d\phi$ and $Nh = r_b - r_p$

Conditions	r_p = 10 (14.1 Debye lengths)					r_p = 100 (141 Debye lengths)				
	Case	$n/(Nh)^2$	$\alpha(Nh)^2$	K	$dF/d\phi$	Case	$n/(Nh)^2$	$\alpha(Nh)^2$	K	$dF/d\phi$
$\phi_p = 10$										
$\phi = 0$	1	1.5	9.4	1.0	2.0	7	1.0	8.0	1.0	2.5
$\phi' = -2\phi/r$	2	4.3	3.0	2.3	2.7	8	5.1	1.8	3.3	3.3
$\phi' = 0$	3	8.2	1.4	3.1	4.5	9	6.2	1.6	3.7	3 3
$\phi_p = 100$										
$\phi = 0$	4	1.0	15	1.0	1.3	10†	5.4	1.3	1.0	16
$\phi' = -2\phi/r$	5	2.7	4.1	1.9	2.4	11	3.5	3.6	2.7	2.0
$\phi' = 0$	6	9.1	1.0	2.7	7.4	12	5.2	2.3	3.4	2.0

*h = 1 for all cases except 10.

†h = 2.5

As a result of the above findings, the following procedure is recommended in order to save computer time when solving similar problems for any chosen boundary condition: First, minimum values of r_b and critical values of α should be found while using large values of h, that is, few grid points. Then h can subsequently be reduced in order to diminish truncation error without the necessity of further changes in r_b and α. It is not yet clear how to choose the proper boundary condition to be used for an arbitrary problem.

An interesting but unjustified assertion has been made by Maslennikov and Sigov (Reference 9) in connection with their use of (2) to iterate the high-velocity satellite wake problem. To ensure stability, the volume of the grid (the region of interest) must be smaller than a number proportional to the ion energy. The present analysis defined Nh to be an appropriate linear dimension of the grid in Debye lengths, and found that $(Nh)^2$ must be less than a certain constant for a fixed α. If X represents the appropriate linear dimension of the grid, and if the effective Debye length is based on the ion directed kinetic energy E_0 (rather than on the electron thermal energy kT), then $(Nh)^2$ is proportional to X^2/E_0. Hence, the criterion is that a cross-sectional area (X^2 rather than the volume X^3 as stated in Reference 9) of the grid must be smaller than a number proportional to E_0: The characteristic energy is the larger of E_0 and kT. Thus, the criterion for stability requires that the dimension X be smaller than a certain number of effective Debye lengths λ^*, where λ^* is defined by $\sqrt{E_0/4\pi n_0 e^2}$ when $E_0 >> kT$ (Reference 9), and by $\sqrt{kT/4\pi n_0 e^2}$ when $E_0 \lesssim kT$.

SECOND ALGORITHM

This section discusses the second algorithm:

$$(L-p)\,\vec{\phi}_{n+1} = \vec{F}(\vec{\phi}_n) - p\,\vec{\phi}_n \tag{7}$$

where p is a scalar relaxation parameter. This extension of the Richardson method (p. 226 of Reference 22, p. 90 of Reference 23) has been studied in connection with mildly nonlinear elliptic equations (References 18 and 19). It will be seen that the iteration properties of (7) are essentially independent of the boundary condition, in contrast to (2). This is because the eigenvalues of L, which contain the boundary condition information, have a minor effect on the spectral radius of the iteration matrix M that relates successive error vectors. By applying a linearization process to (7), similar to that applied to (2),

$$M = (p-L)^{-1}\,(p-J) \tag{8}$$

where J is the Jacobian derivative matrix as in (4). (If the scalar parameter p in (7) were replaced by the matrix J, the linear iteration matrix M would vanish, resulting in a Newtonian-type process, that is, a discrete analog of quasi-linearization (Reference 20).) It is clear that the eigenvalues of J play a crucial role in determining the eigenvalues of M. Assuming the effect of L to be that of a perturbation, then to lowest order the eigenvalues of M are approximated by

$$\lambda = \frac{p-\lambda_J}{p-\lambda_L} \tag{9}$$

where λ_J is an eigenvalue of the Jacobian matrix J, and λ_L is an eigenvalue of the operator L.

It is assumed that the eigenvalues of J are all positive* and lie in the range ($\lambda_1 \leq \lambda_J \leq \lambda_2$). Also, under the conditions leading to (5), all of the λ_L are negative. Hence, for fixed p and λ_J, the largest value of $|\lambda|$ occurs for the minimum value of $-\lambda_L$, which is given by $\lambda_3 = \pi^2/(KN^2h^2)$ when $N >> 1$. Thus, if p is large compared with λ_3, the spectral radius of M, namely σ, becomes independent of the eigenvalues of L and is approximated by

$$\sigma = \frac{\lambda_2}{p} - 1 \qquad \text{for } p < \frac{\lambda_2 + \lambda_1}{2} \tag{10}$$

$$\sigma = 1 - \frac{\lambda_1}{p} \qquad \text{for } p > \frac{\lambda_2 + \lambda_1}{2} \tag{11}$$

Note that, considered as a function of 1/p, $\sigma(1/p)$ is qualitatively similar to $\sigma(\alpha)$ plotted in Figure 1. The minimum value of σ, corresponding to the minimum number of iterations, is

$$\sigma_{min} = \frac{\lambda_2 - \lambda_1}{\lambda_2 + \lambda_1} \tag{12}$$

which occurs when p is equal to the optimum value

$$p_{opt} = \frac{\lambda_2 + \lambda_1}{2} \tag{13}$$

When p exceeds the critical value p_c the spectral radius σ exceeds unity, and the iteration diverges, where

$$p_c = \frac{\lambda_2}{2} \tag{14}$$

Therefore, if the eigenvalues of J are approximately equal (that is, $\lambda_1 \sim \lambda_2$), then $\sigma_{min} << 1$ and $p_{opt} \sim 2p_c \sim \lambda_J$. However, if $\lambda_1 << \lambda_2$,

$$p_{opt} \sim p_c = \frac{\lambda_2}{2} \tag{15}$$

Moreover, if σ is close to unity, then according to (11) the error after n iterations is reduced approximately by the expression $\exp(-n\lambda_1/p)$.

*Justifiable on the basis of analytic forms approximating the space-charge density (Appendix A of Reference 6).

Thus, empirical evaluation of p_{opt} and p_c from iteration experiments with our model problem will give information regarding the eigenvalues of the matrix J for the problem. A check can also be made on the assumptions leading to (5) and (9), and a direct comparison of the two algorithms can be made. Presented in Table 3 are the results of computations using the second algorithm for the same 12 problems presented in Table 1 for the first algorithm. The minimum values of r_b are the same as in Table 1 and are not shown in Table 3. For each case, the table presents five quantities: the optimum value p_{opt}, the range of p containing the critical value p_c, the minimum number n of iterations, the approximate value of λ_2, and the value of $\lambda_4 = 1/\lambda_3$ (the dominant eigenvalue of $-L^{-1}$).

It is evident from Table 3 that p_{opt}, p_c, and the minimum number of iterations are independent of the boundary condition. Actually, for a given r_p and ϕ_p, they depend only on the mesh interval h. Hence, for a given truncation error, governed by h, the two floating conditions require equal numbers of grid points but fewer points than the fixed condition: therefore, the floating conditions are equally economical and are more economical than the fixed condition.

In all cases, the fact that the fractional difference between p_{opt} and p_c is very small is evidence of the validity of (15) and of the inequality $\lambda_1 << \lambda_2$ (assuming (9) to (11) are valid). Hence, from (15) and the empirical values of p_{opt}, λ_2 may be estimated. Now $p_{opt} >> \lambda_3$, where $\lambda_3 = 1/\lambda_4$, in all cases. Therefore, the assumption leading to (9) to (11) is justified, that is, that the effect of L is that of a perturbation. Also, the fact that λ_4 is in all cases larger than λ_2 supports the assumption that the range of the eigenvalues of J is small compared with the range of the eigenvalues of L^{-1}. These considerations apply to h = 1. However, as noted in the footnotes of Table 3, when h was set equal to the small value 0.1 instead of to 1, it was found in Case 1 that p_{opt} was reduced to 0.02, a considerable reduction. Because $p_{opt} << \lambda_3$ in this case, the effect of L can no longer be a small perturbation, so that (9) to (11) are probably invalid. However, the number of iterations was 47, which is approximately the same as for h = 1, which was 52.

Comparison of the numbers of iterations in Table 3 with the corresponding numbers in Table 1 shows that for the given values of h, the second algorithm is more economical than the first. In some cases, the number of iterations is even reduced by an order of magnitude (for example, Case 10). However, the second algorithm is so sensitive to the value of h that the situation can be significantly reversed. For example, for Cases 10 to 12 in Table 3, no satisfactory convergence was obtainable for h = 2.5; that is, the behavior was peculiar in that for p = 90 the current appeared to converge after 5000 to 6000 iterations, but to a value 4 percent lower than that resulting from the first algorithm. For p on either side of 90, however, the iteration number was greater than 25 000, the maximum allowed. Nevertheless, in all cases shown in Tables 1 and 3, the iteration was assumed to have converged properly because both algorithms converged to the same value in every case.

Goddard Space Flight Center
National Aeronautics and Space Administration
Greenbelt, Maryland February 19, 1973
188-48-52-05-51

Table 3

Optimum Iterations with Second Algorithm*

Conditions	r_p = 10 (14.1 Debye lengths)						r_p = 100 (141 Debye lengths)					
	Case	p_{opt}	p_c	n	λ_2 †	λ_4 ‡	Case	p_{opt}	p_c	n	λ_2	λ_4
ϕ_p = 10												
$\phi = 0$	1	1.5§	1.5 to 1.3	52§	3.0	10	7	19	19 to 17	560	38	160
$\phi' = -2\phi/r$	2	1.7	1.7 to 1.6	55	3.4	8.3	8	16	16 to 15	490	32	33
$\phi' = 0$	3	1.7	1.7 to 1.5	55	3.4	11	9	14	14 to 13	430	28	37
ϕ_p = 100												
$\phi = 0$	4	1.7	1.7 to 1.6	390	3.4	48	10‖	62	60 to 58	1000	124	420
$\phi' = -2\phi/r$	5	1.7	1.7 to 1.6	380	3.4	62	11	60	60 to 58	1000	120	240
$\phi' = 0$	6	1.7	1.7 to 1.6	380	3.4	88	12‖	60	60 to 58	1000	120	310

*Tolerance 10^{-5}; h = 1 for Cases 1 to 9.

†$\lambda_2 \equiv 2\, p_{opt} \cong$ largest eigenvalue of matrix J.

‡$\lambda_4 \equiv 1/\lambda_3 = KN^2h^2/\pi^2 \cong$ largest eigenvalue of matrix $-L^{-1}$.

§For h = 0.1, p_{opt} = 0.02 and n = 47.

‖h = 5. Convergence was not satisfactory for h = 2.5.

REFERENCES

1. Laframboise, J. G., *Theory of Spherical and Cylindrical Langmuir Probes in a Collisionless Maxwellian Plasma at Rest*, University of Toronto Institute for Aerospace Studies Report No. 100, June 1966.

2. Bernstein, I. B., and I. N. Rabinowitz, *Phys. Fluids*, 2, 1959, p. 112.

3. Parker, L. W., and E. C. Whipple, Jr., *Ann. Phys.* (USA), **44**, 1967, p. 126.

4. Parker, L. W., *Theory of the Circular Planar (Guardring) Langmuir Probe*, ESSA Technical Report ERL 100-AL2, 1968.

5. Guderley, K. G., and E. M. Valentine, *Theory of Spherical Probes in Monoenergetic Plasmas*, Aerospace Research Laboratories, Wright-Patterson Air Force Base, ARL 65-0024, 1966.

6. Parker, L. W., *Theory of the External Sheath Structure and Ion Collection Characteristics of a Rocket-Borne Mass Spectrometer*, Air Force Cambridge Research Laboratories Report AFCRL-71-0101, 1970.

7. Parker, L. W., *Computer Solutions in Electrostatic Probe Theory*, Air Force Avionics Laboratory Report AFAL-TR-72-222, 1973.

8. Davis, A. H., and I. Harris, *Rarefied Gas Dynamics*, L. Talbot, ed., Academic Press, N. Y., 1961, p. 691.

9. Maslennikov, M. V., and Yu. S. Sigov, *Soviet Physics-Doklady*, **9**, 1965, p. 1063.

10. Call, S., *The Interaction of a Satellite With the Ionosphere*, Ph.D. thesis, Columbia University, 1969.

11. Jew, H., *Numerical Studies of Rarefied-Plasma Interactions at Mesothermal Speeds*, Ph.D. thesis, University of Michigan, 1968.

12. Hamza, V., and E. A. Richley, *Numerical Solution of the Two-Dimensional Poisson Equation*, NASA TND-1323, 1962.

13. Prince, D. C., Jr., and N. P. Jeffries, *Computer Solutions of the Vlasov Equation*, General Electric Final Report, Cincinnati, Ohio, December, 1964.

14. Parker, L. W., and E. C. Sullivan, *Numerical Studies of the Steady-State Plasma Sheath Problem*, Symposium on Computer Simulation of Plasma and Many-Body Problems, NASA SP-153, 1967.

15. Parker, L. W., and E. C. Sullivan, *Rarefied Gas Dynamics*, L. Trilling and H. Y. Wachman, eds., Academic Press, N. Y., 1969, p. 1637.

16. Dupont, T., *SIAM J. Numer. Anal.*, **5**, 1968, p. 753.

17. Coles, W. J., and T. L. Sherman, *SIAM J. Appl. Math*, **15**, 1967, p. 426.

18. Shampine, L. F., *SIAM J. Numer. Anal.*, **5**, 1968, p. 219.

19. Douglas, J., *Numer. Math.*, 3, 1961, p. 92.

20. Bellman, R. E., and R. E. Kalaba, *Quasilinearization and Nonlinear Boundary Value Problems*, Elsevier, N. Y., 1965, Chapt. 5.

21. Bailey, P. B., L. F. Shampine, and P. E. Waltman, *Nonlinear Two Point Boundary Value Problems*, Academic Press, N. Y., 1968.

22. Forsythe, G. E., and W. R. Wasow, *Finite-Difference Methods for Partial Differential Equations*, Wiley, N. Y., 1960.

23. Keller, H. B., *Numerical Methods for Two-Point Boundary-Value Problems*, Blaisdell, Waltham, Massachusetts, 1968.

24. Bohm, D., E. H. S. Burhop, and H. S. W Massey, *Characteristics of Electrical Discharges in Magnetic Fields*, A. Guthrie and R. K. Wakerling, eds., McGraw-Hill, N. Y., 1949, Chapt. 2.

25. Lowan, A. N., *The Operator Approach to Problems of Stability and Convergence*, Scripta Mathematica, Yeshiva University, N. Y., 1957.

26. Taylor, J. C., *Planetary Space Sci.*, **15**, 1967, p. 155.

NASA-Langley, 1974